Spinons and helimagnons in the frustrated Heisenberg chain

Jie Ren[1] and Jesko Sirker[1, 2]

[1]*Department of Physics, Technical University Kaiserslautern, D-67663 Kaiserslautern, Germany*
[2]*Research Center OPTIMAS, Technical University Kaiserslautern, D-67663 Kaiserslautern, Germany*
(Dated: February 24, 2012)

We investigate the dynamical spin structure factor $S(q,\omega)$ for the Heisenberg chain with ferromagnetic nearest ($J_1 < 0$) and antiferromagnetic next-nearest ($J_2 > 0$) neighbor exchange using bosonization and a time-dependent density-matrix renormalization group algorithm. For $|J_1| \ll J_2$ and low energies we analytically find and numerically confirm two spinon branches with different velocities and different spectral weights. Following the evolution of $S(q,\omega)$ with decreasing J_1/J_2 we find that helimagnons develop at high energies just before entering the ferromagnetic phase. Furthermore, we show that a recent interpretation of neutron scattering data for LiCuO$_4$ in terms of two weakly coupled antiferromagnetic chains ($|J_1| \ll J_2$) is not viable. We demonstrate that the data are instead fully consistent with a dominant ferromagnetic coupling, $J_1/J_2 \approx -2$.

Frustrated spin models often show complicated phase diagrams. Apart from phases with conventional (quasi) long-range magnetic order, also valence bond solid, chirally ordered, multipolar as well as spin liquid phases are possible. In addition to identifying and studying the different phases, also the quantum phase transitions between them have attracted considerable interest [1, 2]. Numerical studies are hindered by the so-called sign problem making quantum Monte-Carlo simulations impracticable. Our knowledge about frustrated systems in dimensions $d > 2$ is therefore still limited [3–5]. In one dimension, on the other hand, bosonization techniques can be used to analytically study the weakly frustrated case [6, 7]. Furthermore, with the density-matrix renormalization group (DMRG) [8] a powerful numerical method is available to calculate static properties at zero [6] and finite temperatures [9]. Lately, it has been shown that it is a useful strategy to study frustration in two or three dimensions by a successive coupling of one-dimensional chains [3, 10] thus further motivating investigations of the static and dynamic properties of frustrated spin chains.

The standard spin model to study frustration in one dimension is the $J_1 - J_2$ Heisenberg model

$$H = \sum_j \left[J_1 \boldsymbol{S}_j \boldsymbol{S}_{j+1} + J_2 \boldsymbol{S}_j \boldsymbol{S}_{j+2} \right] \quad (1)$$

with antiferromagnetic coupling $J_2 > 0$. Here $\boldsymbol{S}_j$ is a spin-1/2 operator acting at site j. This model has recently been studied intensely for ferromagnetic coupling $J_1 < 0$ [11–15], driven by the discovery of edge-sharing cuprate chain compounds for which Eq. (1) seems to be the minimal model. These cuprates show fascinating properties including multiferroicity [16–20], i.e., an intricate interplay between incommensurate magnetic and ferroelectric order [21]. It is, however, so far unclear if all of their magnetic properties can be reasonably well described within the simple minimal model (1). In one of the best studied edge-sharing chain cuprates LiCuO$_4$,

for example, susceptibility data seem to point to a dominant ferromagnetic coupling $\alpha \equiv J_1/J_2 \approx -2$ [9, 22] while neutron scattering data have been interpreted in terms of two weakly coupled antiferromagnetic chains $\alpha \approx -0.7$ [23], a conclusion which has later been challenged [24–26].

Apart from being relevant for the edge-sharing cuprate chains, the *dynamical* properties of the $J_1 - J_2$ chain are also of fundamental interest. For $\alpha = 0$ the model consists of two decoupled antiferromagnetic chains whose elementary gapless excitations are spinons. Introducing a small coupling $J_1 < 0$ between the chains leads classically to a spiral magnetic order while bosonization predicts incommensurate spin correlations and an exponentially small gap in the quantum $S = 1/2$ case [7]. At $\alpha_c = -4$ there is an unusual quantum critical point [2] separating the incommensurate from a ferromagnetic phase. Changing the frustration ratio $\alpha \leq 0$ thus turns antiferromagnetic spinons through an incommensurate phase into ferromagnetic magnons.

In this letter we present a systematic study of the dynamical spin structure factor

$$S(q,\omega) = \frac{1}{N} \sum_{j,j'} e^{-iq(j-j')} \int dt\, e^{i\omega t} \langle S_j^z(0) S_{j'}^z(t) \rangle \quad (2)$$

of the J_1-J_2 Heisenberg model (1) from the limit $\alpha = 0$ of decoupled antiferromagnetic Heisenberg chains, across the quantum critical point α_c, into the ferromagnetic phase, $\alpha < -4$. Note that due to $SU(2)$ symmetry it is sufficient to consider the longitudinal correlation function in (2). For $|\alpha| \ll 1$ we compare our data with results obtained by bosonization while for $\alpha \sim -4$ we compare with spin wave theory. Finally, we present a comparison of our results with recent neutron scattering data for the multiferroic cuprate LiCuO$_4$ [23].

We start by considering the weak coupling limit $|\alpha| \ll 1$ by bosonization. On each of the two antiferromagnetically coupled sublattices we write

$$S^z_{2j(+1)} = \sqrt{\frac{K_{1,2}}{\pi}}\partial_x\phi_{1,2} + (-1)^j \mathrm{const}\cos\sqrt{4\pi K_{1,2}}\phi_{1,2}$$

$$S^+_{2j(+1)} \propto \mathrm{e}^{i\sqrt{\frac{\pi}{K}}\theta_{1,2}}\left[(-1)^j + \cos\sqrt{4\pi K_{1,2}}\phi_{1,2}\right]. \qquad (3)$$

Here $\phi_{1(2)}$ are bosonic fields obeying the standard commutation rules $[\phi_\alpha(x),\partial_x\theta_{\alpha'}(x')] = i\delta_{\alpha,\alpha'}\delta(x-x')$ and $K_{1,2}$ are the Luttinger parameters. Let us first consider the free fermion case with $J_2\boldsymbol{S}_i\boldsymbol{S}_j \to \frac{J_2}{2}(S_i^+S_j^- + h.c.)$. Ignoring irrelevant terms, bosonization leads to

$$H = \frac{1}{2}\sum_\alpha \int dx\, v_\alpha \left\{(\partial_x\phi_\alpha)^2 + (\partial_x\theta_\alpha)^2\right\} \qquad (4)$$

for each of the chains $\alpha = 1,2$. In this case $K_1 = K_2 = 1$ and $v_{1,2} = v_F$ with $v_F = 2J_2$ in units of the lattice constant due to a doubling of the unit cell. Apart from irrelevant terms, the interchain coupling J_1 introduces a density-density type interaction

$$H_{d-d} = \frac{2J_1}{\pi}\int dx\,\partial_x\phi_1\partial_x\phi_2\,. \qquad (5)$$

We can absorb this term into the Gaussian part (4) by defining the new fields $\phi_\pm = (\phi_1\pm\phi_2)/\sqrt{2}$ and $\theta_\pm = (\theta_1\pm\theta_2)/\sqrt{2}$. The Hamiltonian (4) stays invariant under this transformation with $\alpha = 1,2$ being replaced by $\alpha = +,-$ but the velocities are renormalized with $v_{1,2} \to v_\pm = v_F \pm J_1/\pi$.

In the isotropic Heisenberg case for $\alpha = 0$ the low-energy properties are still described by (4) but with $v_{1,2} = J_2\pi$ and $K_{1,2} = 1/2$ as known from Bethe ansatz. To keep the $SU(2)$ symmetry intact, we now use non-Abelian instead of the Abelian bosonization (3) for the interchain interaction J_1. This leads to various marginal terms [7, 27] and, in particular, a term which can again be expressed as in (5) but with a different prefactor $2J_1/\pi \to 3J_1/\pi$ leading to a velocity renormalization

$$v_{1,2} = \pi J_2 \to v_\pm = \pi J_2(1\pm 3\alpha/2\pi^2)\,. \qquad (6)$$

The other marginal terms induced by the coupling J_1 have been studied by renormalization group methods in [7] and seem to lead to an exponentially small gap. Numerically, however, no gap in the parameter regime $-4 < \alpha < 0$ has been confirmed yet and we will therefore neglect these terms for the moment.

At weak coupling J_1, the structure factor $S(q,\omega)$ will have low-energy contributions at $q \sim 0,\pi/2,\pi$. We now calculate these contributions in the isotropic case using the free boson Hamiltonian (4) with $\alpha = +,-$ and velocities $v_\pm$ given by Eq. (6). Using the identity (3)—rewritten in terms of $\phi_\pm = (\phi_1\pm\phi_2)/\sqrt{2}$—and the standard result for the boson propagator we obtain

$$S(q\gtrsim 0[\pi - q\lesssim\pi],\omega) \qquad (7)$$
$$\approx Kq(1\pm\cos q)\delta(\omega - v_+q) + Kq(1\mp\cos q)\delta(\omega - v_-q)$$
$$\approx 2Kq\delta(\omega - v_{+[-]}q) + K\frac{q^3}{2}\delta(\omega - v_{-[+]}q)\,.$$

The singularity at $\omega = v_+q$ dominates $S(q\sim 0,\omega)$ while the singularity at $\omega = v_-q$ is dominant for $q \sim \pi$. The other contribution is in both cases supressed by a factor $q^2/4$. Note that $v_+ < v_-$ because $J_1 < 0$. Irrelevant band curvature and interaction terms will lead to a finite linewidth [28, 29], an aspect which is beyond the scope of the present study. For $|k| = |\pi/2 - q| \ll 1$ and v_+, v_- sufficiently different we find

$$S(k,\omega) \propto \theta(\omega - v_+|k|) \qquad (8)$$
$$\times \left\{(\omega^2 - v_+^2 k^2)^{K_- + \frac{K_+}{2} - 1} + |\omega^2 - v_-^2 k^2|^{K_+ + \frac{K_-}{2} - 1}\right\}\,.$$

Here $K_\pm \approx 1/2$ are the Luttinger parameters for the two modes at weak coupling J_1. Note that the divergencies in (8) are weaker than the square-root divergence for the pure isotropic Heisenberg chain [30]. Taking the additional marginal current-current interactions into account perturbatively, we find furthermore an asymmetry $S(\pi/2 - q,\omega) > S(\pi/2 + q,\omega)$ with $q > 0$ small.

To test the analytic predictions in the weak coupling limit and extend our study to the experimentally relevant regime of strong interchain coupling, we now turn to a numerical calculation of the dynamical spin structure factor. We use an adaptive time-dependent density-matrix renormalization group (DMRG) algorithm with a second order Trotter-Suzuki decomposition of the time evolution operator [31]. As time step we choose $J_2\delta t = 0.1$. We present results for an open chain with $N = 400$ sites with 400 states kept in the adaptive Hilbert space. In order to perform the Fourier transform in time in Eq. (2) one has to deal with the problem that numerical data are only available for a finite time interval $t \in [0, t_{\max}]$. The maximal simulation time, $t_{\max} \sim 40J_2$, up to which our numerical results are reliable has been estimated by keeping track of the discarded weight and by comparing with exact results for the XX model and Bethe ansatz results for the isotropic Heisenberg chain [32]. We calculate the spin correlations $\langle S^z_{N/2}(0)S^z_{N/2\pm j}(t)\rangle$. Since two-point spin correlations are negligible for distances much larger than $v_\pm t$, we obtain results almost unaffected by the boundaries in the accessible time interval. These data are then extended in time using linear prediction [33, 34] leading to a smooth exponentially decaying extrapolation of the data. We want to stress that linear prediction does not allow to obtain reliable results for $t > t_{\max}$ but rather represents a smooth cutoff which does not affect the data for $t < t_{\max}$.

In Fig. 1 we show our results for $S(q,\omega)$ for various frustrations. A further check of the quality of the numerical data is obtained by considering the sum rules $I_1 = \int\frac{d\omega}{2\pi}S(q,\omega) = \langle S^z_qS^z_{-q}\rangle$ where $S^z_q = N^{-1/2}\sum_j \mathrm{e}^{-iqj}S^z_j$ and $I_2 = \sum_q I_1 = 1/4$. For all frustrations shown we find that the sum rules are fulfilled with an absolute error of at most 2%. As an example, we show results for I_1 at $\alpha = -2$ in Fig. 2(a).

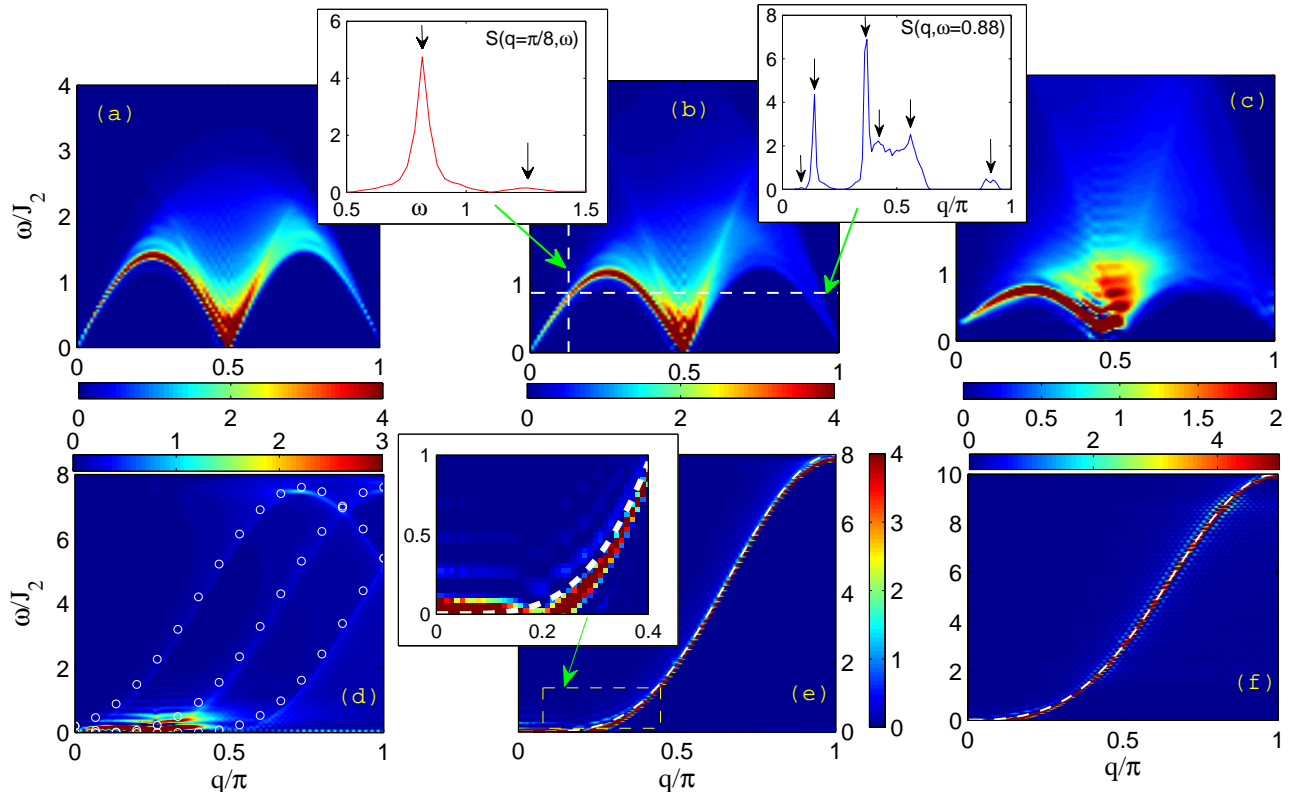For weak frustrations $\alpha = -1/2, -1$ (Fig. 1(a,b)) two

FIG. 1: (Color online) $S(q,\omega)$ for frustrations (a) $\alpha = -1/2$, (b) $\alpha = -1$, (c) $\alpha = -2$, (d) $\alpha = -3.5$, (e) at the quantum critical point $\alpha = -4$, and (f) in the ferromagnetic regime $\alpha = -5$. The insets to (b) show a constant q and constant ω scan with arrows denoting spinon modes discussed in the text. The circles/dashed lines in (d-f) denote the magnon dispersions, Eq. (9).

excitations with different velocities $v_{\pm}$ are clearly visible near $q \sim \pi/2$. As expected from bosonization, the smaller velocity v_{+} agrees with that of the dominant excitation at $q \sim 0$ while the one at $q \sim \pi$ has velocity v_{-}. The velocities extracted from the numerical data also agree fairly well with the prediction from bosonization, see Fig. 2(b). A closer inspection of the data for $\alpha = -1$ also reveals the second mode with velocity v_{-} at $q \sim 0$ with a weight suppressed by approximately $q^2/4$ relative to the dominant mode, see inset of Fig. 1(b).

At larger frustrations the weak coupling picture from bosonization clearly breaks down. For $\alpha = -2, -3.5$ shown in Fig. 1(c) and (d) the low energy spectral weight is concentrated at an incommensurate wave vector q_i. Classically, frustration leads to the formation of a helical state with a pitch vector $Q = \arccos(|\alpha|/4)$. For the quantum model, incommensurate spin correlations have been shown to occur with wave vectors q_i which approach $\pi/2$ with increasing α much faster than in the classical case [9, 11] in full agreement with our dynami-
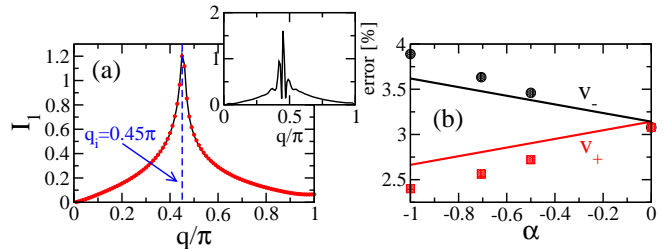

FIG. 2: (Color online) (a) Sum rule I_1 for $\alpha = -2$ from frequency-integrating the numerical data (symbols) compared to a static DMRG calculation (line). The inset shows the absolute error of the frequency-integrated data. (b) Velocities of the elementary excitations $v_{\pm}$. The symbols denote the values extracted from the numerical data for $S(q,\omega)$ at $q \sim 0, \pi$ the lines the prediction from bosonization, Eq. (6).

cal data. For $\alpha = -3.5$ we observe—in addition to the low-energy spectral weight near $q_i \approx 0.26\pi$—the development of three magnon-like dispersions at higher energies.

For the classically expected state with long-range spiral order at wave vector Q, spin-waves have the dispersion

$$\epsilon_q = \sqrt{A_q^2 - B_q^2} \qquad (9)$$

with $A_q = -J_Q + J_q/2 + (J_{q+Q} + J_{q-Q})/4$, $B_q = -J_q/2 + (J_{q+Q} + J_{q-Q})/4$ where $J_q = J_1 \cos q + J_2 \cos 2q$ [35, 36]. In the quantum model, long-range order is destroyed. However, close to the quantum critical point $\alpha_c = -4$ where the model starts to develop a long-ranged ordered ferromagnetic state, the correlation length will become large so that the excitations at high energy remain helimagnon-like. As shown in Fig. 1(d) the helimagnon dispersion (9) does indeed describe the high-energy modes very well with a renormalized effective $\alpha = -3.85$ corresponding to a pitch vector $Q = \arccos(|\alpha|/4) \approx 0.27$. The three modes [35] are then given by ϵ_q and $\epsilon_{q\pm q_i}$ where q_i is the incommensurate wave vector of the *quantum* model.

For $\alpha < -4$ the ground state is a simple ferromagnet, $Q = 0$, and (9) reduces to the magnon dispersion $\epsilon_q = -J_2 \left[(1 - \cos 2q) + \alpha(1 - \cos q)\right]$ which is in excellent agreement with the numerical data as shown in Fig. 1(f). At the quantum critical point, $\alpha_c = -4$, the magnon dispersion becomes quartic, $\epsilon_q = J_2 q^4/2$ at small q. As already noticed in [2] spin-wave theory does not describe the quantum critical point correctly at low energies due to the degeneracy of the ferromagnetic with valence bond solid states [37]. This is confirmed by our data (see inset of Fig. 1(e)) showing that the low-energy spectral weight does not follow the magnon dispersion while the agreement is good at higher energies.

Let us finally discuss our results in the light of recent neutron scattering experiments on LiCuVO$_4$ [23] and LiCuSbO$_4$ [38]. The experimental data for LiCuVO$_4$ have been interpreted in terms of the J_1-J_2 Heisenberg model with $|J_1| < J_2$. However, none of the features predicted by bosonization in this limit and visible in Fig. 1(a,b) have been observed. The neutron data in

Fig. 2 of [23] look instead remarkably similar to our numerical results for $\alpha = -2$. Comparing to the numerically calculated structure factor one has to keep in mind that the neutron scattering data are slightly supressed at higher momenta due to the q-dependence of the atomic form factor for Cu^{2+} ions and the whole spectrum is broadened due to a finite q, ω resolution. However, this does not affect the qualitative features of the spectrum. In fact, we can even obtain a quantitatively satisfying description of the data, see Fig. 3. For small momenta the agreement becomes excellent when convoluting the numerical data with a Gaussian to take the finite instrumental resolution into account. A frustration $\alpha \sim -2$ implies an incommensurate wave vector $q_i \approx 0.45\pi$, see Fig. 2(a), consistent with the neutron data and susceptibility measurements [9, 22]. For such a strong frustration the explanation of the spectral weight at high energies in terms of multispinon excitations of the antiferromagnetic chains offered in Ref. [23] is not viable. Instead, this weight is related to the incommensurate spin correlations in this material caused by the dominant ferromagnetic coupling between the chains. Let us also briefly comment on very recent neutron scattering results on powder samples of LiCuSbO$_4$ [38]. The powder averaging prevents a detailed analysis, however, the concentration of spectral weight at the incommensurate wave vector $q_i \approx 0.47\pi$ points again to a strong frustration $\alpha \approx -2$ which is fully consistent with an analysis of susceptibility and specific heat data [38].
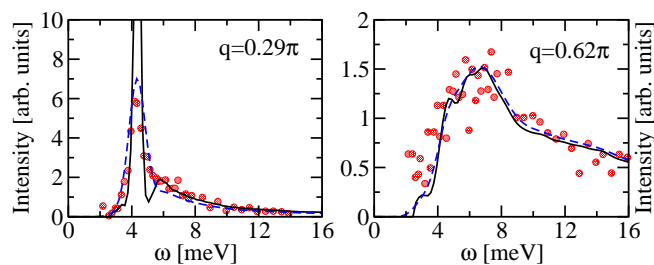
FIG. 3: (Color online) Neutron scattering data taken from Fig. 3 of Ref. [23] (circles) compared to the DMRG data with $J_2 = 6$ meV and $\alpha = -2$ (solid lines). The dashed lines are the same DMRG spectra broadened by convoluting with a Gaussian with a FWHM of 1.1 meV. The height of the theoretical spectra has been scaled to fit the data best.

[1] T. Senthil, A. Viswanath, L. Balents, S. Sachdev, and M. P. A. Fisher, Science **303**, 1490 (2004).
[2] J. Sirker, V. Y. Krivnov, D. V. Dmitriev, A. Herzog, O. Janson, S. Nishimoto, S.-L. Drechsler, and J. Richter, Phys. Rev. B **84**, 144403 (2011).
[3] S. Yan, D. A. Huse, and S. R. White, Science **332**, 1173 (2011).
[4] J. Sirker, W. Zheng, O. Sushkov, and J. Oitmaa, Phys. Rev. B **73**, 184420 (2006).
[5] H.-C. Jiang, H. Yao, and L. Balents, arXiv:1112.2241 (2011).
[6] S. R. White and I. Affleck, Phys. Rev. B **54**, 9862 (1996).
[7] A. Nersesyan, A. Gogolin, and F. H. L. Essler, Phys. Rev. Lett. **81**, 910 (1998).
[8] S. R. White, Phys. Rev. Lett. **69**, 2863 (1992).
[9] J. Sirker, Phys. Rev. B **81**, 014419 (2010).
[10] M. Kohno, O. A. Starykh, and L. Balents, Nat. Phys. **3**, 790 (2007).
[11] R. Bursill, G. A. Gehring, D. J. J. Farnell, J. B. Parkinson, T. Xiang, and C. Zeng, J. Phys: Cond. Mat. **7**, 8605 (1995).

[12] T. Hikihara, L. Kecke, T. Momoi, and A. Furusaki, Phys. Rev. B **78**, 144404 (2008).

[13] J. Sudan, A. Lüscher, and A. M. Läuchli, Phys. Rev. B **80**, 140402(R) (2009).

[14] T. Vekua, A. Honecker, H.-J. Mikeska, and F. Heidrich-Meisner, Phys. Rev. B **76**, 174420 (2007).

[15] F. Heidrich-Meisner, A. Honecker, and T. Vekua, Phys. Rev. B **74**, 020403(R) (2006).

[16] T. Masuda, A. Zheludev, A.Bush, M. Markina, and A. Vasiliev, Phys. Rev. Lett. **92**, 177201 (2004).

[17] S. Park, Y. J. Choi, C. I. Zhang, and S.-W. Cheong, Phys. Rev. Lett. **98**, 057601 (2007).

[18] S. Seki, Y. Yamasaki, M. Soda, M. Matsuura, K. Hirota, and Y. Tokura, Phys. Rev. Lett. **100**, 127201 (2008).

[19] S.-L. Drechsler, O. Volkova, A. N. Vasiliev *et al.*, Phys. Rev. Lett. **98**, 077202 (2007).

[20] F. Schrettle, S. Krohns, P. Lunkenheimer, J. Hemberger, N. Büttgen, H.-A. Krug von Nidda, A. V. Prokofiev, and A. Loidl, Phys. Rev. B **77**, 144101 (2008).

[21] H. Katsura, N. Nagaosa, and A. V. Balatsky, Phys. Rev. Lett. **95**, 057205 (2005).

[22] N. Büttgen, H.-A. Krug von Nidda, L. E. Svistov, L. A. Prozorova, A. Prokofiev, and W. Aßmus, Phys. Rev. B **76**, 014440 (2007).

[23] M. Enderle, B. Fak, H.-J. Mikeska, R. K. Kremer, A. Prokofiev, and W. Assmus, Phys. Rev. Lett. **104**, 237207 (2010).

[24] S.-L. Drechsler, S. Nishimoto, R. O. Kuzian, J. Málek, W. E. A. Lorenz, J. Richter, J. van den Brink, M. Schmitt, and H. Rosner, Phys. Rev. Lett. **106**, 219701 (2011).

[25] S. Nishimoto, S.-L. Drechsler, R. Kuzian, J. Richter, J. Malek, M. Schmitt, J. van den Brink, and H. Rosner, arXiv: 1105.2810 (2011).

[26] M. Enderle, B. Fak, H.-J. Mikeska, and R. Kremer, Phys. Rev. Lett. **106**, 219702 (2011).

[27] D. Allen and D. Sénéchal, Phys. Rev. B **55**, 299 (1997).

[28] R. G. Pereira, J. Sirker, J.-S. Caux, R. Hagemans, J. M. Maillet, S. R. White, and I. Affleck, Phys. Rev. Lett. **96**, 257202 (2006).

[29] R. G. Pereira, J. Sirker, J.-S. Caux, R. Hagemans, J. M. Maillet, S. R. White, and I. Affleck, J. Stat. Mech. P08022 (2007).

[30] H. J. Schulz, Phys. Rev. B **34**, 6372 (1986).

[31] A. E. Feiguin and S. R. White, Phys. Rev. B **72**, 220401(R) (2005).

[32] J.-S. Caux, R. Hagemans, and J. M. Maillet, J. Stat. Mech. P09003 (2005).

[33] T. Barthel, U. Schollwöck, and S. R. White, Phys. Rev. B **79**, 245101 (2009).

[34] G. U. Yule, Philo. Trans. R. Soc. London Ser. A **226**, 267 (1927).

[35] T. Nagamiya, *Solid State Physics: Advances in Research and Applications* (Academic Press, New York, 1967), p. 305.

[36] M. E. Zhitomirsky and I. A. Zaliznyak, Phys. Rev. B **53**, 3428 (1996).

[37] T. Hamada, J. Kane, S. Nakagawa, and Y. Natsume, J. Phys. Soc. Jpn. **57**, 1891 (1988).

[38] S. E. Dutton, M. Kumar, M. Mourigal, Z. G. Soos, J.-J. Wen, C. L. Broholm, N. H. Andersen, Q. Huang, M. Zbiri, R. Toft-Petersen, et al., arXiv:1109.4061 (2011).